Scanning Microscopy

Volume 2 | Number 2 Article 11

12-12-1987

Microanalytical and Micromorphological Investigations of High Temperature Materials With and Without Protective Coatings

Volker Thien
Siemens AG, Group KWU

W. Voss
Siemens AG, Group KWU

Scanning Microscopy, Vol. 2, No. 2, 1988 (Pages 747-766)
Scanning Microscopy International, Chicago (AMF O'Hare), IL 60666 USA

0891-7035/88$3.00+.00

MICROANALYTICAL AND MICROMORPHOLOGICAL INVESTIGATIONS OF HIGH TEMPERATURE MATERIALS WITH AND WITHOUT PROTECTIVE COATINGS

V. Thien* and W. Voss

Siemens AG, Group KWU, Materials Technology,
Mülheim-Ruhr, Federal Republic of Germany

(Received for publication May 04, 1987, and in revised form December 12, 1987)

Abstract

The phenomenon "High Temperature Corrosion" (HTC) is described; three different types (pure oxidation, high temperature hot corrosion, low temperature hot corrosion) are defined. HTC is demonstrated taking gas turbine blades as an example. The results of laboratory HTC tests under defined conditions were compared with those of long time engine experience; the agreement is very satisfactory.

Metallurgical investigations with scanning electron microscopy and EDX-/WDX-analytical techniques gave explanations for the behaviour of protective coatings. The corrosion mechanism of a NiCrAlY-plasma spray coating is explained as consequence of Cr- and Al-oxidation. A special analytical technique - the "integral layer profile analysis" - is introduced to ameliorate concentration profile methods. By examining IN 738 LC specimen with CoCrAlY-plasma spray coating, stressed by hot gas at 900°C, the limits of this system are shown.

The aim of the present work is to demonstrate how the analytical techniques mentioned can contribute to the selection of materials and protective coatings leading to higher rentability, higher output and durability of the plant.

KEY WORDS: High Temperature Materials, High Temperature Corrosion, Coatings, Laboratory and Operation Tests, Method "Integral Layer Profile Analysis" with Energy-dispersive and Wavelength-dispersive X-ray Analysis Systems, Materials Characterization up to 900°C.

*Address for correspondence:
Volker Thien, Siemens AG, Group KWU, Abt. TWCP, Postfach 10 17 55, D-4330 Mülheim-Ruhr, Federal Republic of Germany Phone No. 49-208-456-2800

Introduction

High Temperature Materials are defined as those materials, of which the operation temperature is permanently at or above 700°C (after Dienst [10]). Typical fields of application are, e.g., automotive engines, high temperature reactors, apparatus of chemical industry plants, and gas turbines for aircraft engines and power plants (stationary gas turbines), as well. In the present paper, the application of High Temperature Materials for blades of stationary gas turbines is used to demonstrate to which extent microanalytical investigations can influence the selection and qualification of materials themselves and the characterization of protective coating systems; a prospect for the near future is also given. Damage due to High Temperature Corrosion (HTC) reduces the efficiency and endangers the safety of energy plant components, e.g., gas turbines. Some research programs have been carried out at international and national levels [17,22,23]. Several types of high temperature corrosion phenomena encountered cannot be described in detail in this paper. Numerous investigations to clarify HTC-processes on a microscopic scale, using methods as electron-beam microanalysis, transmission and scanning electron microscopy and special analytical methods, e.g., Auger electron spectroscopy (AES), secondary ion mass spectrometry (SIMS) have been published [1,3-6,9-13, 15,17.18], including our work [24-32]. The new results of recent investigations are also presented here (see "Microanalytical Investigations"). The blades of gas turbines are highly stressed components, subject to erosive and corrosive influences and thermo-mechanical stresses. The required properties are provided by complex Ni- and Co-base alloys (see Table 1

and references [25,28,31]); HTC is the main factor limiting the lifetime. Numerous metallurgical investigations, mainly under HTC conditions, have been carried out and their results have been compared with those of long time engine experience. In recent years, the inlet temperatures have been continuously increased to achieve greater output and efficiency. Also, the propensity to High Temperature Corrosion (HTC) has increased [2, 11,28]. This required intensive investigations, carried out in national and international programs (cf. later on: High Temperature Corrosion). To limit the HTC attack on blade materials, several protective coatings have been developed and investigated (cf. the literature survey and citations further on). An important point is here also the ability of refurbishing [16]. The present paper reports investigations to realize protective coating/base material combinations being resistant to HTC for long times.

Table 1: Base Materials, used in Laboratory and Operation Tests

Material	Alloy Type	Chemical Composition in %															
		Ni	Cr	Co	Mo	W	Ta	Nb	Al	Ti	Fe	Mn	Si	C	B	Zr	Y
Nickel-Base-Alloys																	
U 520	Forged	57	19	12	6	1	–	–	2	3	–	–	–	.05	.005	–	–
U 500	Cast	52	18	19	4.2	–	–	–	3	3	–	–	–	.07	.007	.05	–
IN 738 LC	Cast	61	16	8.5	1.7	2.6	1.7	.90	3.4	3.4	–	–	–	.17	.01	.10	–
IN 939	Cast	48	22.5	19	–	2	1.4	1	1.9	3.7	>.50	>.20	>.20	.15	.01	.10	–
Cobalt-Base-Alloys																	
S 816	Cast	20	20	42	4	4	–	4	–	–	4	1.2	.40	.38	–	–	–
FSX 414	Cast	10	29	52	–	7.5	–	–	–	–	1	–	–	.25	.01	–	–
FSX 418	Cast	10	30	52	–	7	–	–	–	–	1	–	–	.25	–	–	.15

Table 2: Protective Coatings, used in Laboratory and Operation Tests

Type of Coating	Procedure	Chemical Composition in %							
		Si	Al	Cr	Mo	Ni	B	Co	Y
Chromised	Diffusion			45–80					
Aluminised	Diffusion		≈ 30						
Chrome-Aluminised	Diffusion		30	15–35		25–37			
L DC 2	Diffusion	Duplex-Coating: Pt – Al							
Elcoat 360	Diffusion	Duplex-Coating: Ti – Si							
Ni Cr Al Y (ATD 1)	Plasma Spray (Vacuum)		11	38		Balance			0.25
Co Cr Al Y (ATD 2)	Plasma Spray (Vacuum)		12.5	25				Balance	0.35
Ni Co Cr Al Y (LN 20)	Plasma Spray (atmosphere)		7.5	29		41		22	0.5
Co Cr Al Y	Plasma Spray (atmosphere)		13	23				Balance	0.6
Ni Cr Si Mo B	Plasma Spray (atmosphere)	4		16	2	70	3		

High Temperature Corrosion Phenomena

In general, High Temperature Corrosion (HTC) is defined as damage due to oxidation and sulfidation of metallic materials by hot gas and other solid and fluid components. The extremely large number of possible corrosive media results in different forms of layers, attacks, and chemical reactions. Dependent on the material temperature, the following ranges of HTC are roughly characterized (as shown schematically in Figure 1a):

a) Pure oxidation ($T \geq 950^{\circ}C$).
b) HTC Type I (High temperature hot corrosion) at temperatures $\geq 750^{\circ}C$, with a maximum at about $850^{\circ}C$. Here, reactions of the metals of the base materials occur because of the oxygen and sulphure content of the fuel gas; mainly sulphides (preceding sulfidation) and oxides (preceding oxidation) are formed.
c) HTC Type II (Low temperature hot corrosion) at temperatures $\geq 650^{\circ}C$. [7,8,19] Reactions with the material surface lead to low melting eutectics - e.g., alkali sulphates -, which attack the material, forming a damage of greater area.

Another important type of HTC attack is the catastrophic oxidation caused by vanadium. The various mechanisms of HTC have been extensively discussed in the literature [3-6,13,14,18,21,33,34] and in a recent volume edited by Rahmel [20]. Base materials and protective coatings show a specific good or bad resistance against the different types of corrosion. As given in Figure 1b, a material A has good resistance against oxidation, but bad against HTC type I and II; material B is resistant against HTC I, but not against HTC II and oxidation, whereas material C has good resistance against HTC II, but a bad one against HTC I and oxidation. An optimized material - as indicated - should have satisfying resistance against HTC I and II, rather bad properties against oxidation. Thus, a combination base material-coating must be adapted to the operating conditions.

In Figure 2, a survey is presented about the influencing factors on the system component-coating and the interaction between base material-coating-environment, respectively.

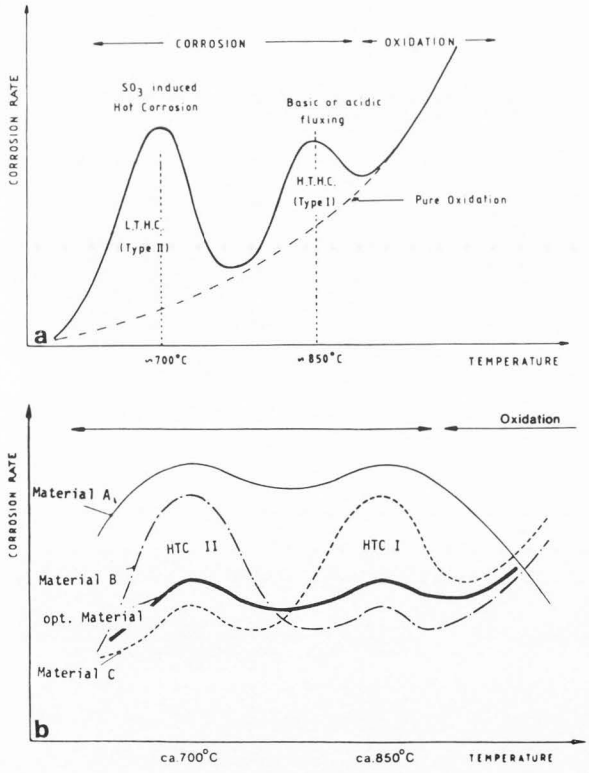

Fig. 1. High Temperature Corrosion (HTC). a) Schematic representation of different types; b) resistance of different coatings and base materials against HTC (scheme).

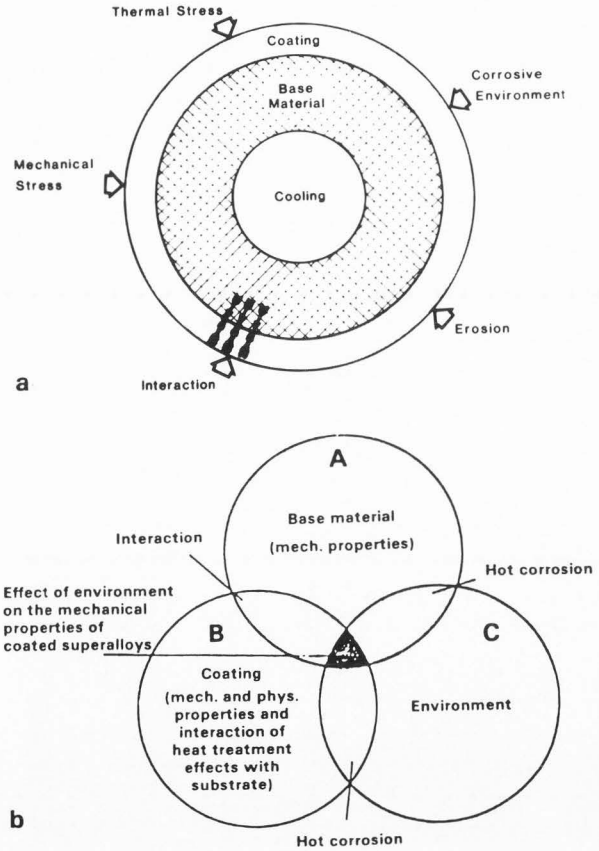

Fig. 2. Factors determining effectiveness of coating. a) Substrate and coating; b) substrate, coating and environment.

Materials and Methods

The materials used in this work and their chemical composition are shown in Table 1. Samples for laboratory HTC tests of 15 mm diameter and 3 mm height have been tested under synthetic ash and in air with 0.03 Vol.% SO_2/SO_3 additives at various temperatures and running times. Also, coated materials have been tested in the same way; chemical composition and application processes of the coatings used are given in Table 2.

Creep rupture samples have been tested in hot gas rigs under defined mechanical stress [28,31,32]. The same materials were used in a set of vanes and stationary blades, respectively, in a gas turbine, fired with natural gas (cf. further on: Results). Specimens were taken out of the components and examined in the same way.

Metallographic investigations: Cross-sections of base material and chromized coatings were polished and etched in Kalling's solution (2 g Cu-chloride, 80 cm^3 ethyl alcohol, C_2H_5COOH, 40 cm^3 HCl); those of plasma spray coatings were etched in 10 % Adler solution (a) 3 g $CuNH_4Cl_3$ dissolved in 25 cm^3 demineralized water, (b) 15 g Fe_3Cl dissolved in 50 cm^3 HCl; then both solutions combined.

Electron beam microanalysis has been carried out on a Siemens Elmisonde; the scanning electron microscopy was performed on a Camscan DV4 with Microspec-WDX 2A wavelength-dispersive X-ray analysis system und Tracor Northern 5500/5600 energy dispersive X-ray analysis system.

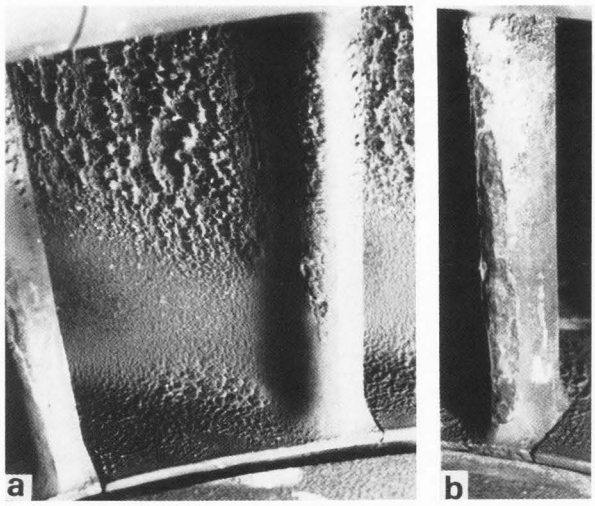

Fig. 3. HTC-Manifestation. Stationary blades, row 1; process gas, coal gasification. Material: Udimet 520, chromized. a) With deposits; b) deposits removed.

HTC-Manifestations on Blade Materials, Laboratory and In-Service Tests

In Figure 3a, the operation results of a gas turbine fired with process gas (coal combustion gas to achieve higher output mixed with fuel oil) are represented. In spite of the rather low temperature (T = 600°C), a first attack could be recognized already after 1,000 h operation time; the attack was much heavier after 10,000 h. The layer analysis pointed out - at 30 % - a part of heavy metals (Pb, Sn, Sb, Cd) indicating an aggressive sulphate melt. The effect of a protective coating is as an example shown in Figure 4 on an attack of fuel oil on running blades (material: Nimonic 90) for more than 30,000 h.

The unprotected blade has a serious attack, starting from corrosion pits; from the metallographic investigation, along a section A-B, a sulfidation, running in advance, can be seen. Such a sulphide attack on a blade is also shown in Figure 5. The material was Udimet 520, subjected to natural gas, containing sulphur, for approximately 27,000 h at 750°C. The results of metallographic and microprobe investigations are shown in the partial images; a section was made along the line A-B, presented as overview in Figure 5b

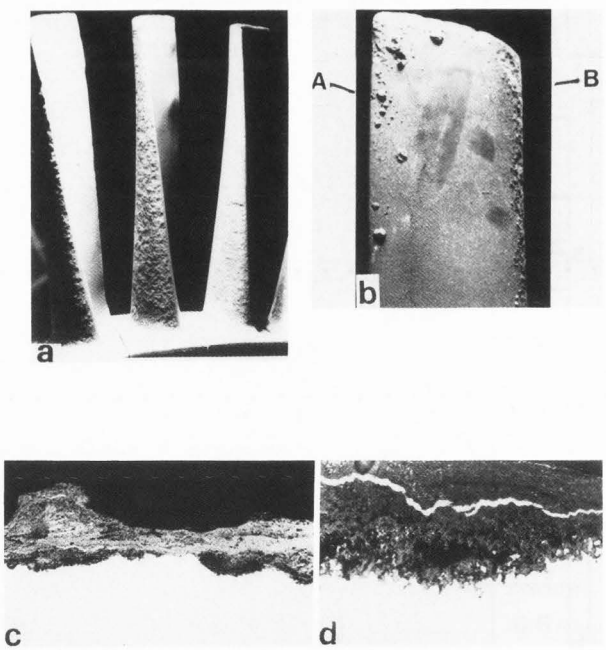

Fig. 4. HTC-Manifestation. Stationary blades, row 1: fuel oil EL. Material: Nimonic 90. a) 1 = uncoated blade, 2 = chromized; b) corroded uncoated blade; c) microsection along A-B; d) detail from c).

and a metallographic investigation (detail I) in Figure 5c. The microprobe results in Figure 5d show very clearly the distribution of the most important elements in the outer zones (analysis made perpendicular to segment of 5c).

As a comparison with laboratory results, various materials and protective coatings were used in a set of vanes (and also in the first row of rotating blades) of a gas turbine, fired with natural gas. At regular intervals, these blades were examined. In Figure 6, a schematic view of the distribution of coated (marked 1) and uncoated alloys in a vane row is given; by comparing the HTC behaviour

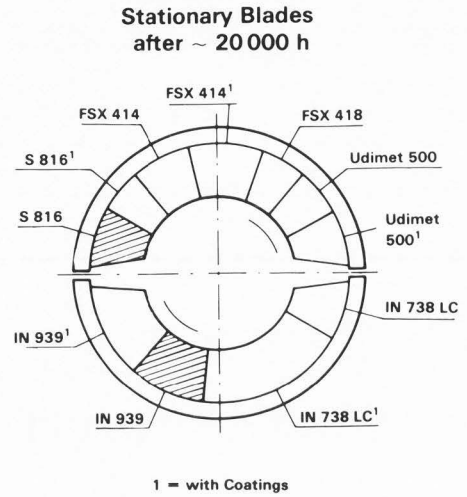

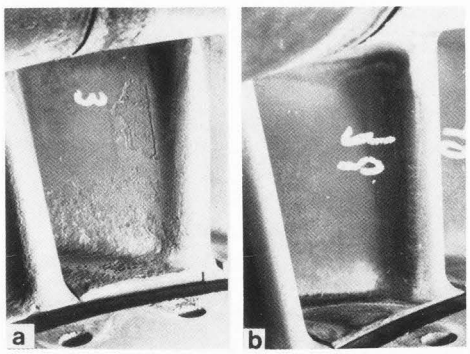

Fig. 6. HTC in-service tests. Mixed blade set (vanes); circle indicates alloy distribution. Comparison after 20,000 h, 750°C, natural gas with S-content. a) Alloy S 816, heavy attack; b) IN 939, no greater attack. (above)

Fig. 7. HTC in-service tests. Rotating blades; 10,000 h, 750°C, natural gas with S-content. Circle indicates distribution of coatings. Base material: Udimet 520. a) Uncoated, considerable attack; b) coated (Cr-diffusion), no attack. (right)

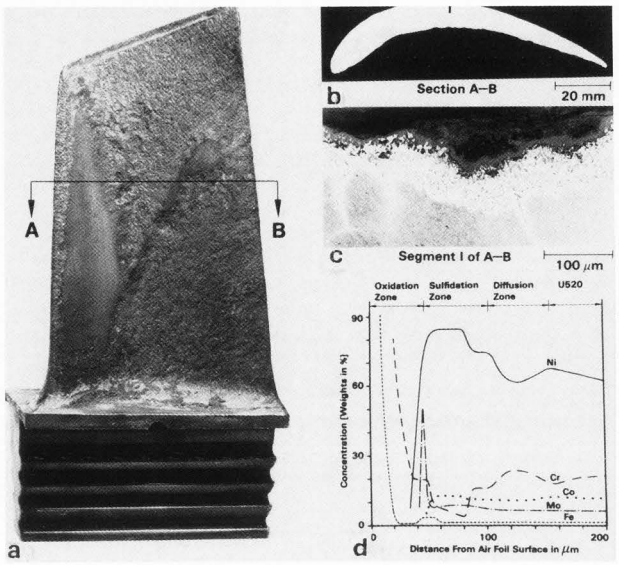

Fig. 5. High temperature corrosion on a gas turbine blade. a) Blade after 27,293 h; b) section A-B as indicated; c) microsection at position I; d) corresponding element distribution.

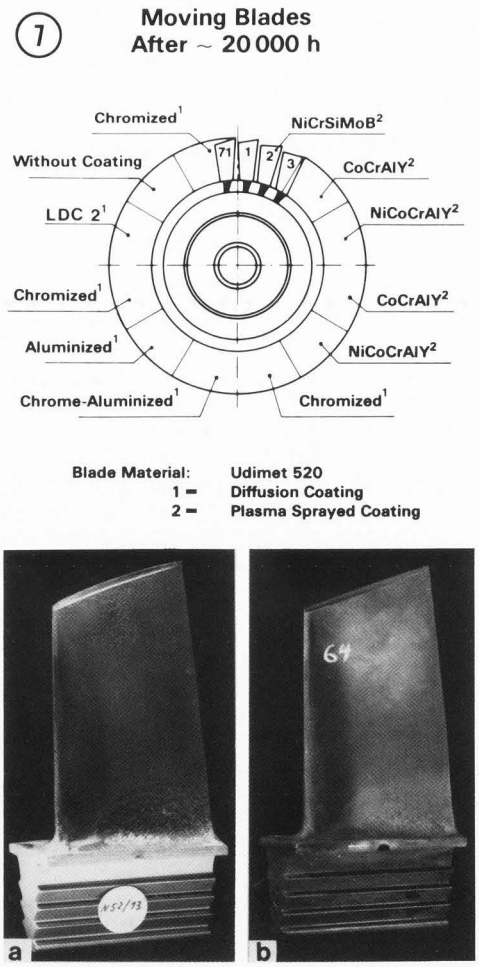

after 20,000 h operating time of the alloys S 816 -Figure 6a - and IN 939 - Figure 6b -, the laboratory results are confirmed. Comparable results were achieved also after 40,000 h. The effect of various protective coatings is demonstrated for example in Figure 7. The circle indicates the choice of coating type (diffusion or plasma sprayed; base material: Udimet 520); the uncoated version - Figure 7a - shows considerable HTC attack, whereas at the coated blade - Figure 7b - no attack can be recognized.

Protective Coatings Against High Temperature Corrosion

Two different procedures are mainly applied; one way is the diffusion method to enrich the surface of the base alloy with additional elements, the other is the plasma spray method. With diffusion methods, diffusing elements can combine with alloying elements to form new phases resistant to HTC. One advantage is that diffusion coatings generally have a homogeneous connection to the base material and only lead to slight alteration in the dimension of the component [25,28, 29,31]. As an important element to form a layer of Al_2O_3 on the surface, Al is preferably used; generally in combination with other elements, e.g., Cr serving as protection against alkaline sulphate corrosion.

As mentioned above, a number of coatings of different composition and manufacturing procedure has been tested in long time experiments in a gas turbine fired with natural gas, and the results are compared to those of laboratory tests. In Figure 8, the compilation of data which we got from our work is represented in a column diagram; as a criterion, the time until (macroscopically visible) penetration was chosen. The first in-service inspection was after 5,000 h so that in some cases the results of laboratory tests would have been closer to those from operational testing. The group of Cr-diffusion coatings (first three in Figure 8) showed the best behaviour against HTC (under the given conditions); from the plasma spray coatings, NiCrAlY type showed relatively good resistance.

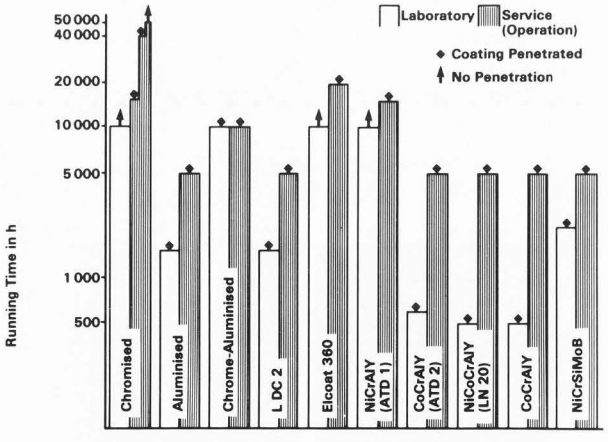

Fig. 8. HTC-resistance. Comparison of various coating systems on base material Udimet 520 (cf. Table 2). Vertical axis: running time (logarithmic scale). Laboratory (white columns) and operation results (shadowed column). First five systems: diffusion coatings; others: plasma spray coatings.

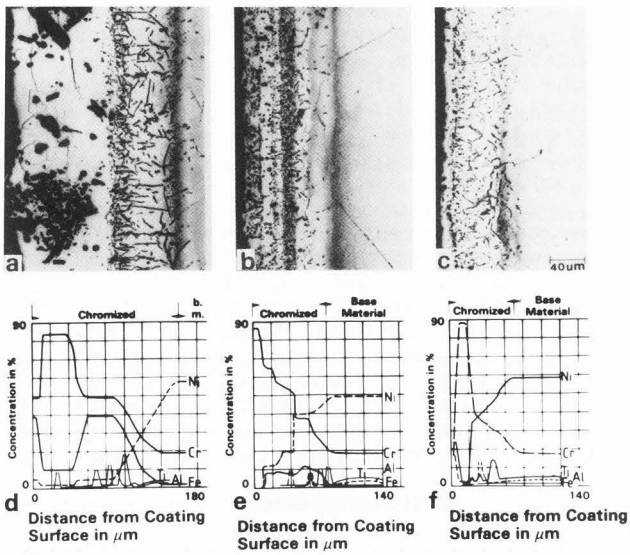

Fig. 9. Comparison of Cr-diffusion coatings of different suppliers; a,b,c): Polished cross-sections etched with Kalling's solution; d,e,f): Corresponding element distribution (microprobe analysis). Arrow indicates oxide clusters.

Microanalytical Investigations of Coating Systems

Chromized (Chromium-Diffusion) Coatings

Similar coatings from three different suppliers, indicated as types I, II and III, were examined. Figure 9 contains in the upper part cross-sections of these coatings in the initial state. Coating type I (Figure 9a) shows rod-shaped Al-oxides, situated in clusters (see arrow). These clusters easily lead to micro-cracks and weaken the effectiveness of the coating. Running times were reached between 15,000 and 55,000 h, depending on the number of inhomogeneities; average lifetime was about 20,000 to 25,000 h. In coating type II (Figure 9b), the oxides

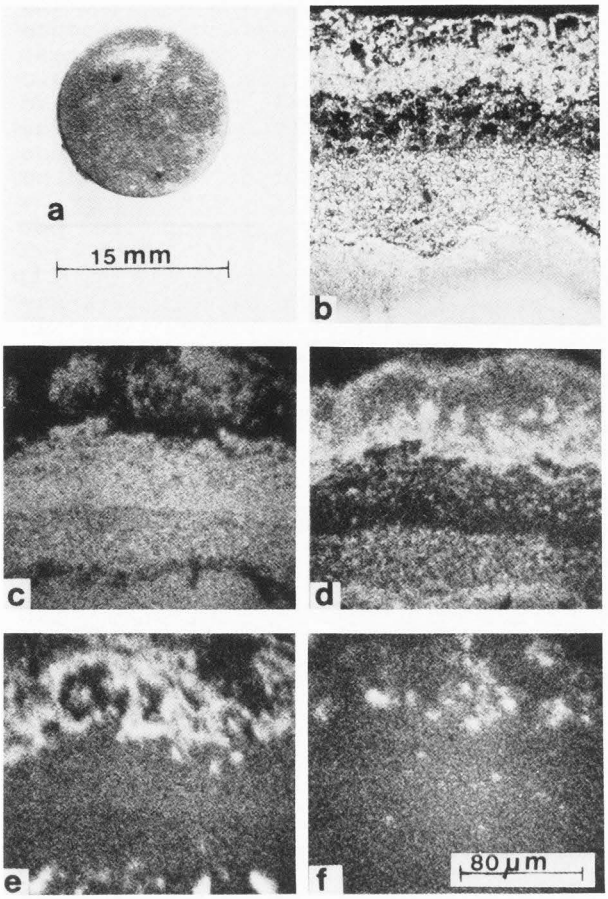

Fig. 10. HTC-laboratory test of plasma spray coating NiCrAlY on base material Udimet 520. a) Sample (small cylinder) after test (10,000 h); macroscopic view; b) cross-section perpendicular to surface (random); X-ray element maps (microprobe): c) Ni; d) Cr; e) Al; f) S.

have a uniform distribution; this coating reached 55,000 h operating time with no macroscopic visible penetration. Coating type III (Figure 9c) has comparable microstructure but lower thickness (from Figure 9f, 20 µm compared to 40 µm for type II, Figure 9e). First penetration occurred after 15,000 h. The coating was useless after 20,000 h; obviously the thickness was not sufficient. In Figures 9d, e, f, the elemental distribution profiles (by electron beam microanalysis) of the coatings are shown. The change of layer composition for the elements Cr, Al, Ti, Ni results in prevention of alkaline sulphate corrosion up to the lifetime mentioned.

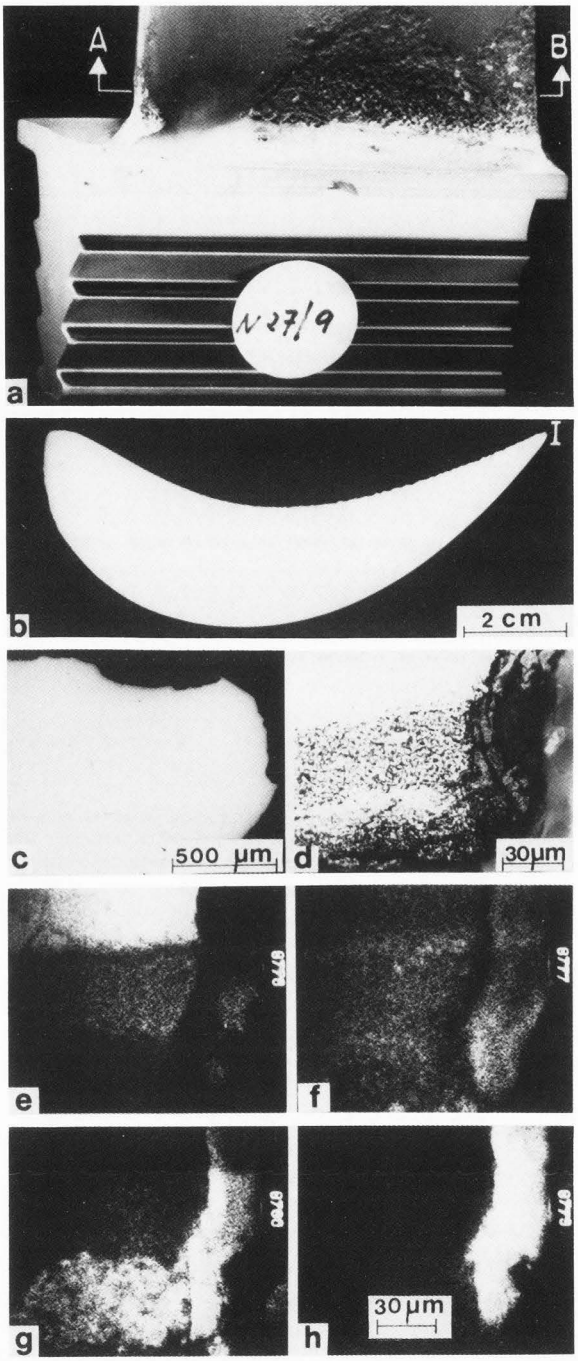

Fig. 11. Rotating blade, material Udimet 520, with NiCrAlY plasma spray coating after 20,000 h operation. a) Blade, lower part; b) section along A-B, as indicated; size relation to (a) given; c) microsection position I, survey, and d) detail. Element distribution maps: e) Ni; f) Cr; g) Al; h) S.

Plasma Spray Coatings

These coatings must be applied under vacuum; because in the presence of air, oxides are formed which then serve as initiation for corrosion attack (selective oxidation after short times). As an example of plasma spray coatings, results on a NiCrAlY-coating are compared from laboratory and in-service tests.

Figure 10a shows a sample exposed to HTC conditions (synthetic ash, air + 0.03 Vol.% SO_2/SO_3) for 10,000 h. In this figure, an attack - but not a severe damage - can be recognized on the surface. From microanalytical investigation, shown by X-ray elemental maps, Figures 10c, d, e, f, corresponding to the cross-section, Figure 10b, as a consequence of HTC, a Cr- and Al-oxide layer appeared closer to the surface; the outward diffusion of Cr results in its decrease in the center; correspondingly, the Al- and Ni-contents increase here. At times, S-containing particles are distributed in the inner oxide layer. The behaviour of this NiCrAlY-coating after operation of 20,000 h in acidic natural gas is given in Figure 11. A rotating blade (material Udimet 520) showed symptoms of corrosive attack at its lower part. A section was prepared (along A-B), Figure 11b, and an area marked I (exactly at the trailing edge) was examined by microanalysis. A corrosion product had remained at this place; the elemental distribution maps (high amounts of Cr, Al, S) indicate the presence of Cr- and Al-oxides and Cr-sulphides. From the Cr-distribution the original duplex coating composition can be inferred. Oxidation penetrates the layer from the outside; Cr has relatively uniform distribution, Al has a higher concentration close to the surface. Al-oxides are widely spread in the coating; whereas a S-influence is only weakly recognizable (S-signal has been very amplified!). The corrosion mechanism is assumed to be as follows: at first, a Cr-oxide layer is formed with little Al-participation. After the decrease in Cr-content, oxidation of Al takes place by outward diffusion of Al. Sulphur plays only a role when the coating has failed (fully oxidized).

The Method of "Integral Layer Profile Analysis"

In our above mentioned investigations, the phenomenon HTC has been described exemplarily on selected material-coating combinations for gas turbine blades mainly in the temperature region up to T = 750°C (Material-Surface-Temperature). In consequence to these results, the question was to answer how far higher gas inlet and/or higher material surface temperature would influence the HTC-behaviour. In hot gas test rigs - at the Technische Hochschule Darmstadt, FRG [31,32] -, the Ni-base alloy IN 738 LC has been tested under mechanical stress at temperatures up to 900°C; as coating system, the plasma spray layer CoCrAlY - cf. Table 2 - has been chosen. The hot gas was fuel oil EL with corrosive additives (0.5 % S, 15 ppm Na, 10 ppm Cl, 5 ppm V). Figure 12 gives ED-X-ray element distribution images of Ni, Co, Cr and Al; Ni - main element in the base alloy - is not present in the coating layer; the border base material-coating can be remarked easily by comparing Co- and Ni-distribution.

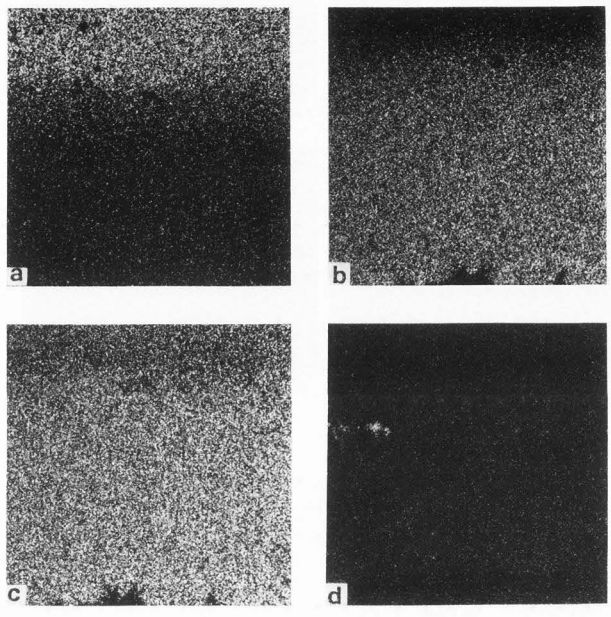

Fig. 12. Hot gas test specimen. Material: IN 738 LC with CoCrAlY plasma spray coating. As-received condition; element distribution (X-ray) maps: a) Ni; b) Co; c) Cr; d) Al.

Procedure and Results; IN 738 LC with CoCrAlY Coating

In general, the concentration of elements is measured microanalytically by means of line-scans (characteristic X-ray intensity along a chosen line). This procedure has the disadvantage that local fluctuations of concentration - like inclusions or defaults - accidentally lead to misinterpretations. Otherwise, smaller concentration changes cannot be displayed by X-ray maps because of their limited detectability.

This can be avoided by the procedure of "integral layer profile analysis", mentioned by the authors in a recent work [32].

The method is as follows (cf. Figure 13a): Selected specimen areas (analytical windows, here 10 µm x 140 µm) were investigated with the EDX-system using a standardless semi-quantitative analysis program. By moving the specimen in steps of 10 µm, 30 of those stripes were analysed side by side; the X-ray intensities were corrected also with a ZAF-program. In Table 3, a listing of those concentration values of 10 elements is represented; Figure 13b demonstrates the concentration profiles of Co, Cr, Al and Ni; the heat treatment during the coating process results in a slight outward diffusion of Ni.

In the same manner, a specimen out of the hot gas test rig was examined after 1,523 h of attack. The metallographic examination is shown in Figure 14 in a survey and two micro-sections; the micro-image of the opposite side (direction of gas outflow) reveals a dual composition of the layer: -phase (Cr-rich, light) and -phase (Co-, Al-rich, dark). The corresponding distribution images - Figure 15 - show a low enrichment of Ni in the coating, whereas Co and Cr are mainly represented; the oxygen distribution indicates an oxidation attack. In Figure 16, a comparison between a SEM-image of the exposure side - coating/base material - and the corresponding concentration profiles are given (in Figure 16a, an analytical window is exemplarily shown). The outward diffusion of Ni is remarkable; the profiles of Cr and Al have great

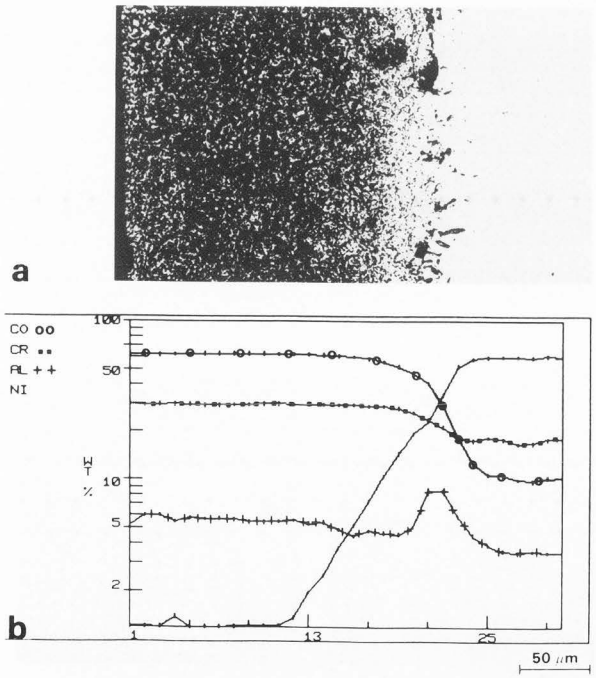

Fig. 13. "Integral layer profile analysis" (same specimen as Fig. 12). a) SEM-images; b) concentration profiles of Co, Cr, Al, Ni.

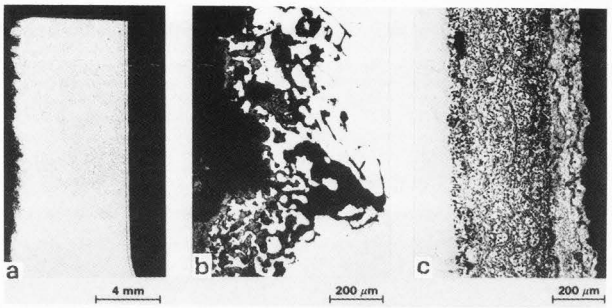

Fig. 14. HTC-creep test specimen: IN 738 LC and CoCrAlY coating. Fuel with corrosive additives, 900°C, σ = 130 N/mm², 1,523 h. Metallographic examination. a) Survey; b) exposure side, unetched; c) opposite side (outflow); Kalling's etchant.

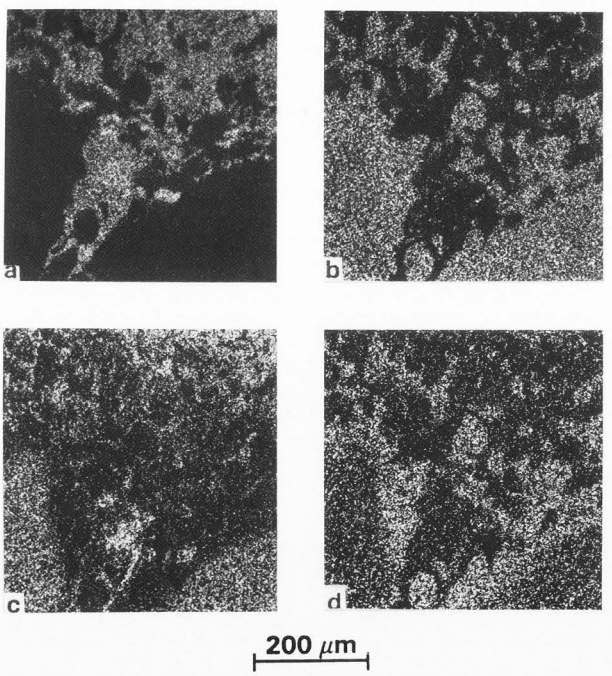

Fig. 15. Same specimen as in Fig. 14. Direction of outflow. Investigation with SEM/WDX: (X-ray maps) a) O; b) Ni; c) Co; d) Cr.

alterations; at the surface, Cr is enriched up to 40 %, Al has a 40 % peak in 40 µm depth.

Effect and process of HTC-attack can be recognized very clearly at a specimen broken in the hot gas test rig after 1,702 h. As shown in the metallographic examination - Figure 17 -, a heavy HTC-attack takes place along the grain boundaries in the base material; correspondingly, this attack is represented by the SEM-images of Figure 18. The element distributions (WD-Analysis) of oxygen and sulphur - (cf. the comparable shape!) - indicate the preceding sulfidation and oxidation along grain boundaries, as mentioned several times in the literature.

In confirmation to that, a BSE-image (showing differences in atomic number) was made in comparison to the concentration maps of Al, Ni, Co (EDX) and S, O (WDX), respectively (Figure 19). Sulphur and oxygen are widely spread towards the base material, Ni has a strong outward diffusion, Cr a diminuation in the outer layer; the coating has obviously lost its effectiveness to a great extent.

This situation is shown very distinctly in the integral layer profile analysis, Figure 20. Co has extreme alterations in the coating, but is enriched (inward-diffusion) over a certain distance in the base material. The Cr-concentration behaviour is especially complicated; there is a complete loss along a distance of 300 µm into the base material, until the base material value is reached. Al shows a similar behaviour, but its loss distance is only 100 µm.

In Figure 21, a comparison of the three different specimen conditions is given. The progressive HTC-attack of fuel oil EL at T = 900°C demonstrates that the coating system CoCrAlY on

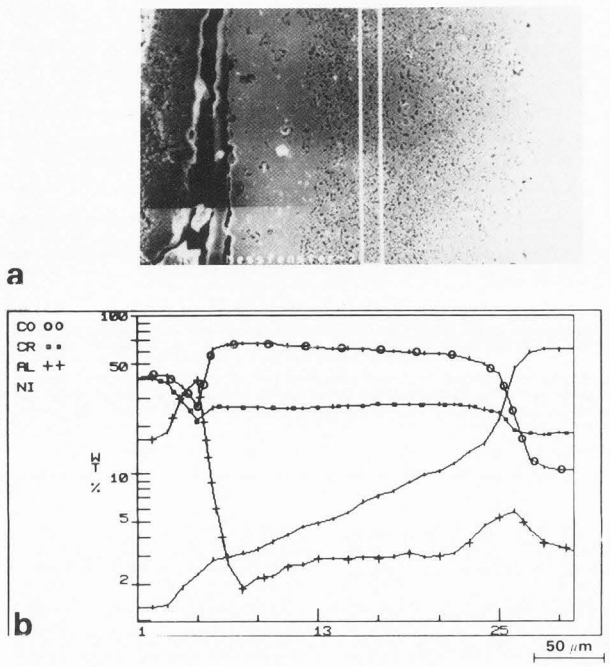

Fig. 16. Same specimen as in Fig. 14. Integral layer profile analysis. a) SEM-image with analytical window; b) concentration profiles Co, Cr, Al, Ni.

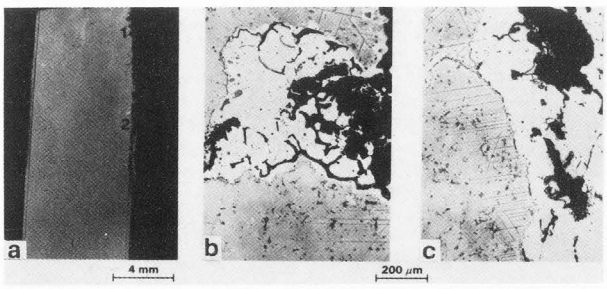

Fig. 17. HTC-creep test specimen; IN 738 LC/CoCrAlY-coating. Time to fracture 1,702 h, 900°C, = 130 N/mm². Metallographic investigation. a) Survey; b,c) microsections 1, 2 as indicated.

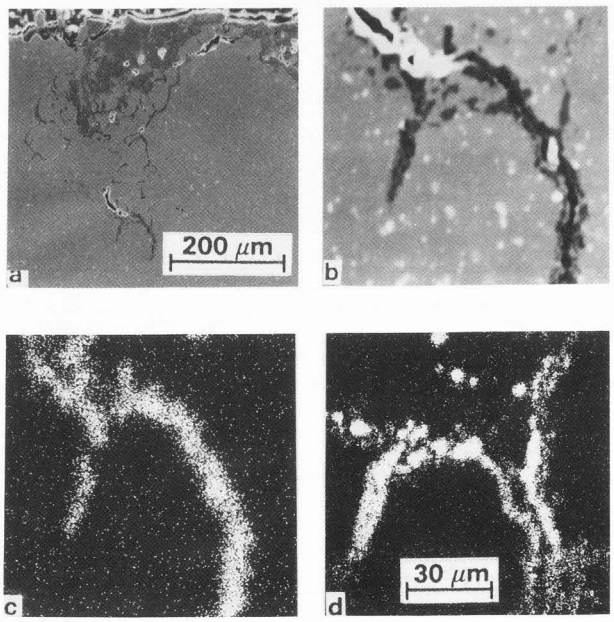

Fig. 18. SEM/WDX examination, specimen as in Fig. 17. a) SE-image, total view; b) SE-image, partial view; c) O-X-ray map; d) S-X-ray map. Note preceding sulfidation/oxidation along grain boundaries.

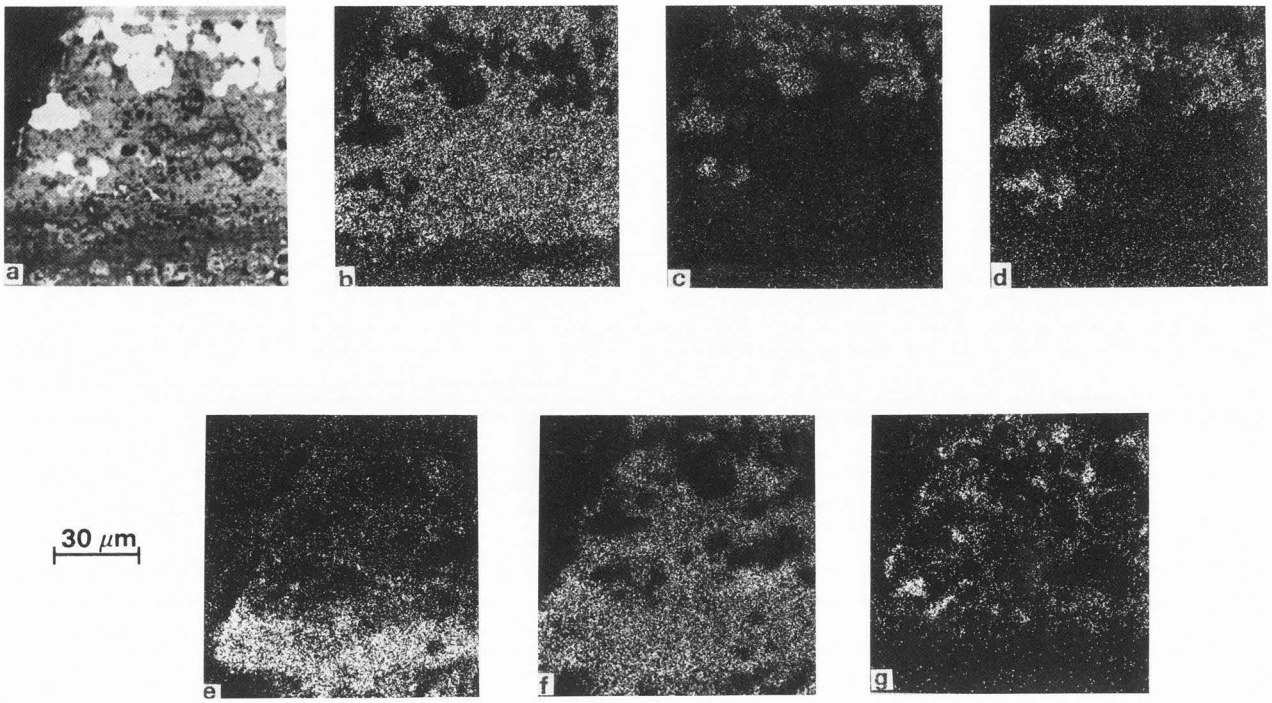

Fig. 19. HTC-creep test specimen as in Fig. 17. SEM/X-ray analysis investigation. a) Backscattered electron image (atomic number contrast); b) -e) EDX-concentration maps of Cr, Co, Ni, Al; f,g) WDX-concentration maps of O and S.

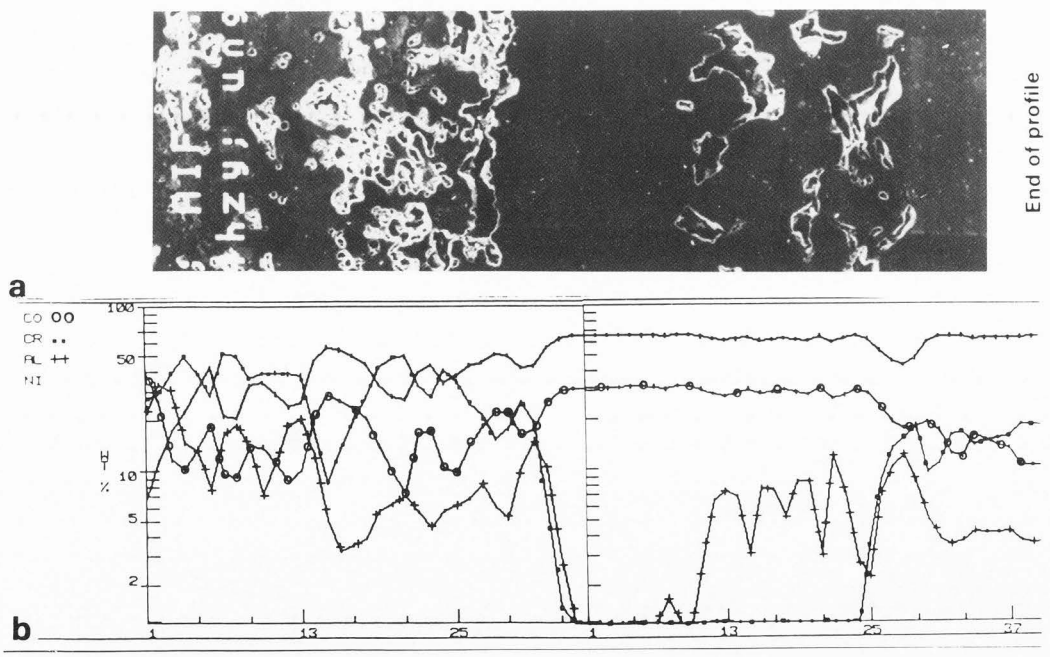

Fig. 20. HTC-creep test specimen as in Fig. 17. a) SE-image, coating/base material, hot gas attack from the left; b) "integral layer profile analysis" of Co, Cr, Al, Ni.

IN 738 LC - which has shown a very good performance at temperatures $t \leq 800^{\circ}C$ - is not suitable under these conditions; either another coating system must be taken, or the material temperature must be lowered (e.g, by inner cooling systems).

The direct HTC-attack in the hot gas rigs is obviously more aggressive as even the conditions in a gas turbine. Some laboratory test procedures carried out some years ago correspond better with the real lifetimes. As an example, the element concentration profiles of a specimen of IN 738 LC with CoCrAlY-coating are compared in Figure 22 in the as-delivered condition and after a laboratory test under synthetic ash and hot air ($850^{\circ}C$) with additives (0.03 Vol.% SO_2/SO_3) for 2,000 h. There are no serious changes in the element concentrations; a Ni outward-diffusion could be expected. Thus, the evaluation of the hot gas test rig results must be regarded with a certain correction factor in respect to the engine behaviour.

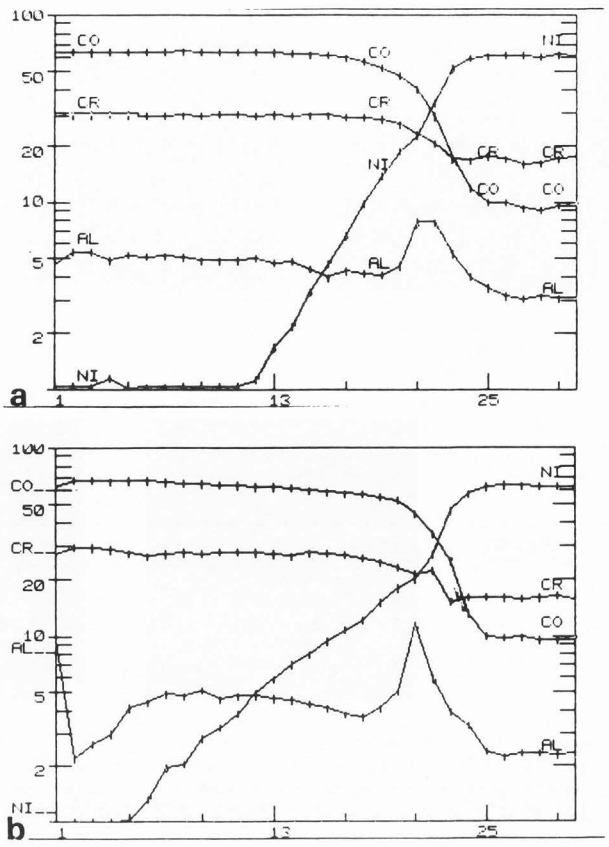

Fig. 22. IN 738 LC + CoCrAlY-coating. Analysis procedure "integral layer profile". a) As-received; b) after HTC-laboratory test, 2,000 h/$850^{\circ}C$, synthetic ash, hot air with 0.03 Vol.% SO_2/SO_3. (above)

Fig. 21. Analytical procedure "integral layer profile analysis", concentration profiles of elements Co, Cr, Al, Ni. HTC-creep test specimen IN 738 LC, coating CoCrAlY. a) As-received; b) after hot gas attack, 1,523 h/$900^{\circ}C$, direction of outflow; c) after hot gas attack, 1,702 h/$900^{\circ}C$, incident direction (slight difference of dimension of abscissa caused by technical reasons). (left)

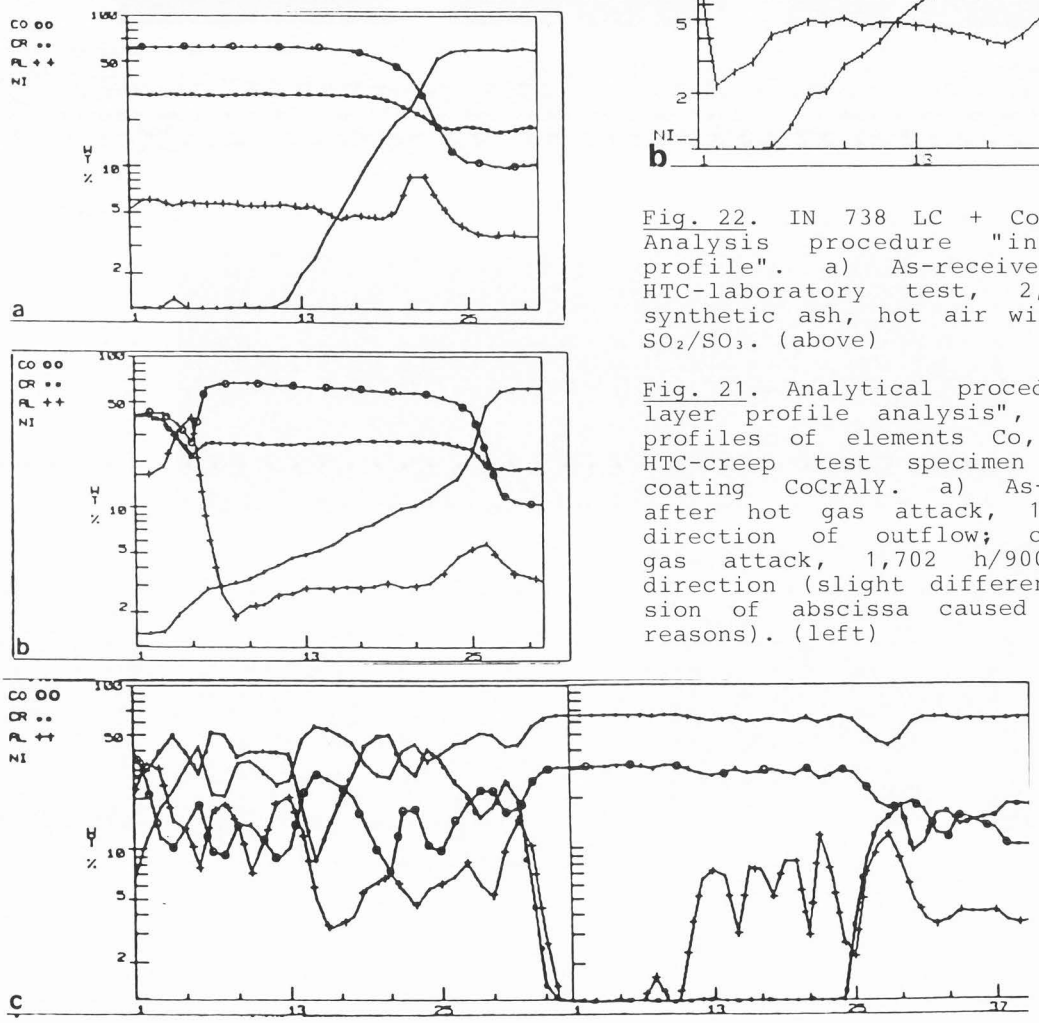

Udimet 520 with NiCrAlY Coating

The technique of "integral layer profile analysis" has also been carried out at a number of other combinations of base material and coating. As an example, this is demonstrated with specimen of the forged alloy Udimet 520 with NiCrAlY (see also Tables 1 and 2). In Figure 23, a microsection of the border coating/base material is shown, with the WDX-element distribution of Ni and Cr, which indicates the duplex composition of the coating. These results are also shown by the concentration profiles in Figure 24. Cr has its maximum at and near the surface, followed by the Ni maximum, as expected from the concentration maps. The "crossing" between Al and Co indicates approximately the position of the transition area. The same combination has been examined after a laboratory test of 10,000 h at 750°C, under synthetic ash, hot air and additives of SO_2/SO_3. Figure 25 shows a partial view in a SEM-image; the X-ray maps reveal that the duplex composition Cr/Ni is still present, but oxygen - obviously forming Cr- and Al-oxides - has penetrated into greater parts of the coating; also sulphur appears in the same region.

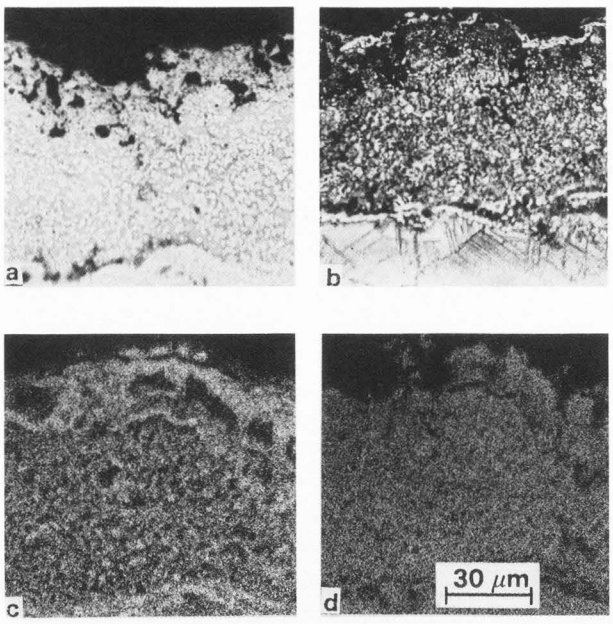

Fig. 23. HTC-laboratory test, specimen of alloy Udimet 520 with NiCrAlY plasma spray coating, as-received. Border coating/base material. a) Metallographic examination unetched; b) etched with Kalling's etchant; c) Cr-distribution (WDX); d) Ni-distribution (WDX).

The inward-diffusion of Al is also represented in the concentration profiles of Figure 26; the mentioned duplex composition Cr/Ni is underlined by the local consequence of Cr- and Ni-maxima. The rather good condition of the coating relates to the slight changes in the concentration profiles.

These results are in very good agreement to those of operation tests in a gas turbine, fired with natural gas [cf. "Manifestations of HTC" and 27,28,31]. A blade of such a material/coating combination was examined after 20,000 h in-service time - see Figure 27 -; a section along a line A-B was made and investigated in the same way. As demonstrated by the X-ray maps of Figure 28, Al-oxides have formed at the surface, and an Al-diffusion towards the base material has

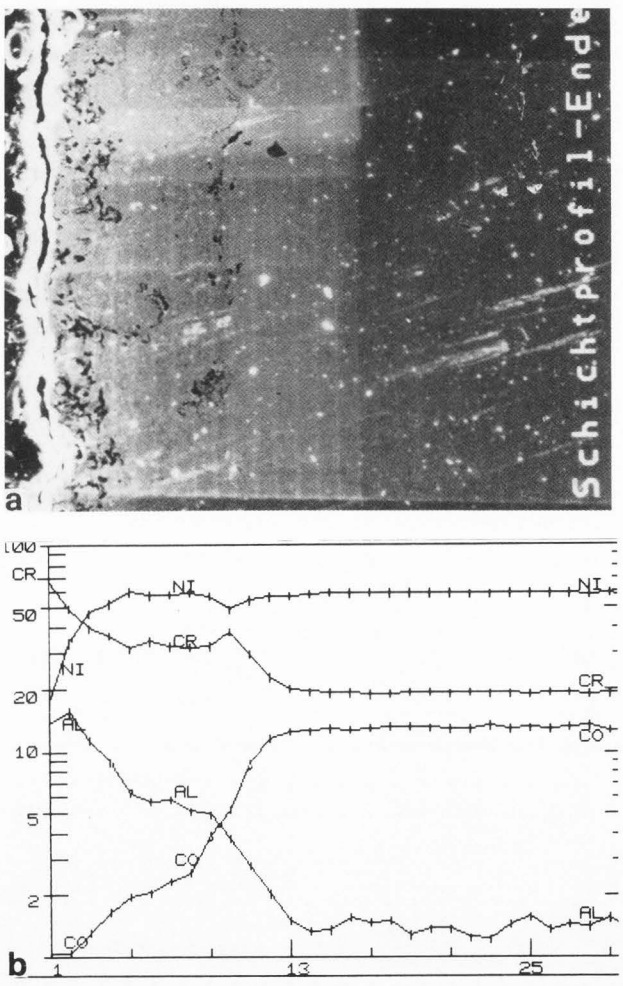

Fig. 24. "Integral layer profile analysis", specimen as in Fig. 23. a) SE-image, border coating/base material; b) corresponding concentration profiles of Co, Cr, Ni and Al.

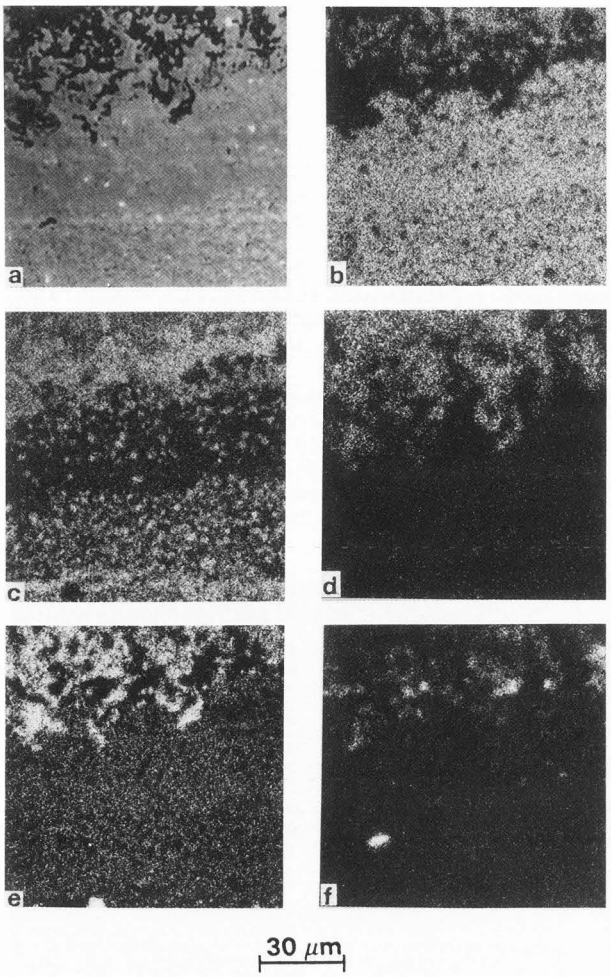

Fig. 25. HTC-laboratory test. Udimet 520 with NiCrAlY-coating, synthetic ash, 750°C/10,000 h, hot air with 0.03 Vol.% SO_2/SO_3, SEM/WD-X-ray examination. a) SE-image; b) - f) WD-X-ray maps of Ni, Cr, O, Al, S.

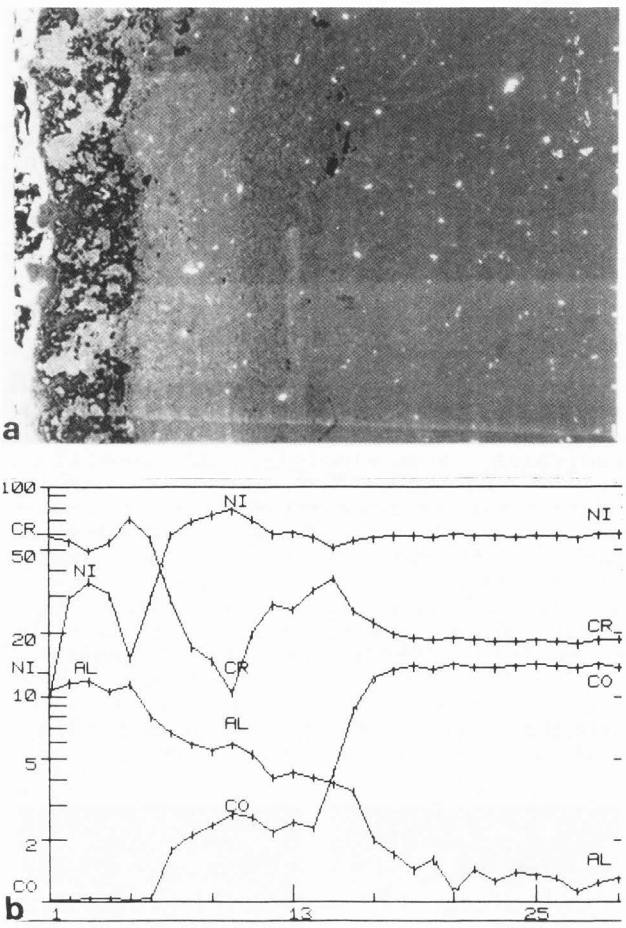

Fig. 26. "Integral layer profile analysis", specimen as in Fig. 25. a) SE-image; b) concentration profiles of Co, Cr, Ni, Al. Note dual composition of layer (spatial distance between Ni and Cr-peak)!

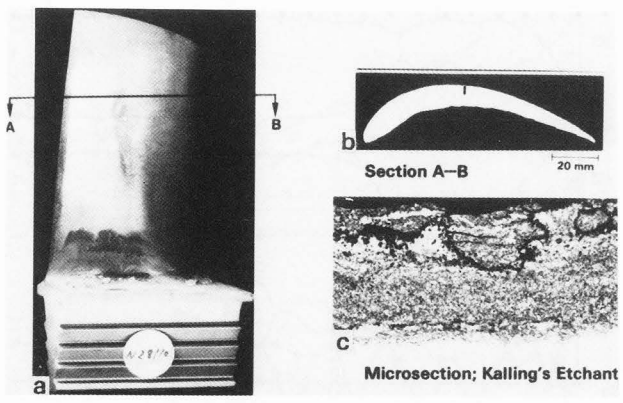

Fig. 27. HTC-in-service test. Blade material Udimet 520 with NiCrAlY plasma spray coating, 20,000 h/750°C, natural gas. a) Survey; b) section along A-B, as indicated; c) microsection, using Kalling's etchant.

taken place, also an outward diffusion of Ni, which has separate maxima from those of Cr. A stronger attack of sulphur cannot be stated; also, the concentration profile of Figure 29 - corresponding to the SEM-image - indicates that HTC has influenced the system coating/base material until a depth of 200 µm, and considerable changes in the concentration of the main elements have occurred, but - and that is the result of the comparison in Figure 30 - not in a severe manner. By comparing the as-delivered condition with the HTC laboratory test and the in-service blade, the effectiveness of this combination (under these conditions!) and the transferability of the laboratory test results to real relations in a gas turbine can be proved.

Table 3. Integral Layer Profile Analysis; element concentrations at 30 positions 10 µm steps; material: Udimet 520 with NiCrAlY-coating.

FILE LABEL: TWCP2-1070-PROFIL
WEIGHT% DATA FOR POINTS 1 TO 30

POINT	AL-K	S-K	MO-L	CA-K	TI-K	CR-K	FE-K	CO-K	NI-K	ZN-K	TOTAL
1	13.67	0.00	6.90	1.34	0.19	27.11	4.85	0.72	28.83	16.39	100.00
2	16.39	0.00	4.62	0.97	0.16	34.88	1.98	0.46	28.75	11.79	100.00
3	17.57	3.68	0.00	0.58	0.00	41.56	0.57	0.63	31.01	4.58	100.02
4	12.60	0.00	2.64	0.31	0.04	29.10	0.31	1.09	52.49	1.42	100.00
5	8.03	0.46	0.00	0.07	0.06	24.95	0.31	1.17	64.70	0.25	100.00
6	8.73	0.00	2.85	0.12	0.00	32.05	0.15	1.27	54.75	0.00	100.00
7	11.69	0.18	0.23	0.21	0.04	48.06	0.33	1.18	38.00	0.00	100.00
8	11.96	0.00	6.30	0.16	0.01	47.46	0.19	1.17	32.59	0.15	99.99
9	13.63	0.00	5.97	0.20	0.06	39.96	0.23	1.76	38.17	0.00	99.98
10	13.03	0.00	3.10	0.12	0.07	31.49	0.23	2.33	49.62	0.00	99.99
11	9.83	0.00	1.42	0.00	0.11	25.27	0.16	1.77	61.11	0.26	100.01
12	9.18	1.02	0.00	0.15	0.10	23.17	0.34	1.82	64.21	0.00	99.99
13	8.87	3.22	0.00	0.10	0.06	19.36	0.24	1.86	66.25	0.02	99.98
14	6.26	0.00	0.00	0.02	0.03	17.37	0.33	1.97	73.14	0.00	100.00
15	4.66	0.00	1.85	0.14	0.11	21.79	0.23	1.57	69.64	0.00	99.99
16	4.56	0.00	1.10	0.07	0.38	30.65	0.15	1.08	62.01	0.00	100.00
17	4.17	0.00	4.96	0.11	0.40	28.99	0.12	1.01	60.24	0.00	100.00
18	5.60	0.00	3.41	0.12	0.96	24.40	0.20	1.29	64.02	0.00	100.00
19	8.76	0.00	5.67	0.07	1.22	30.59	0.02	1.46	44.21	0.00	100.00
20	7.24	1.35	0.00	0.16	1.19	40.19	0.20	2.45	47.14	0.00	100.00
21	2.85	3.13	0.00	0.20	1.63	24.54	0.35	7.21	60.09	0.00	100.00
22	1.72	4.84	0.00	0.04	2.78	21.24	0.11	11.75	57.60	0.00	100.00
23	1.51	3.37	0.44	0.06	3.02	20.17	0.31	12.78	58.35	0.00	100.01
24	1.33	7.61	0.00	0.06	2.93	18.96	0.23	12.41	56.47	0.00	100.00
25	1.34	2.91	0.76	0.03	2.98	19.27	0.31	12.89	59.50	0.00	99.99
26	1.36	2.69	1.33	0.00	2.87	19.42	0.00	13.15	59.18	0.00	100.00
27	1.32	4.42	0.00	0.17	2.84	19.20	0.18	12.96	58.90	0.00	99.99
28	1.16	3.32	0.36	0.00	3.00	19.46	0.12	13.34	59.24	0.00	100.00
29	1.18	5.24	0.00	0.15	2.98	19.04	0.25	12.82	58.33	0.00	99.99
30	1.37	4.77	0.00	0.01	2.92	19.38	0.02	13.10	58.43	0.00	100.00

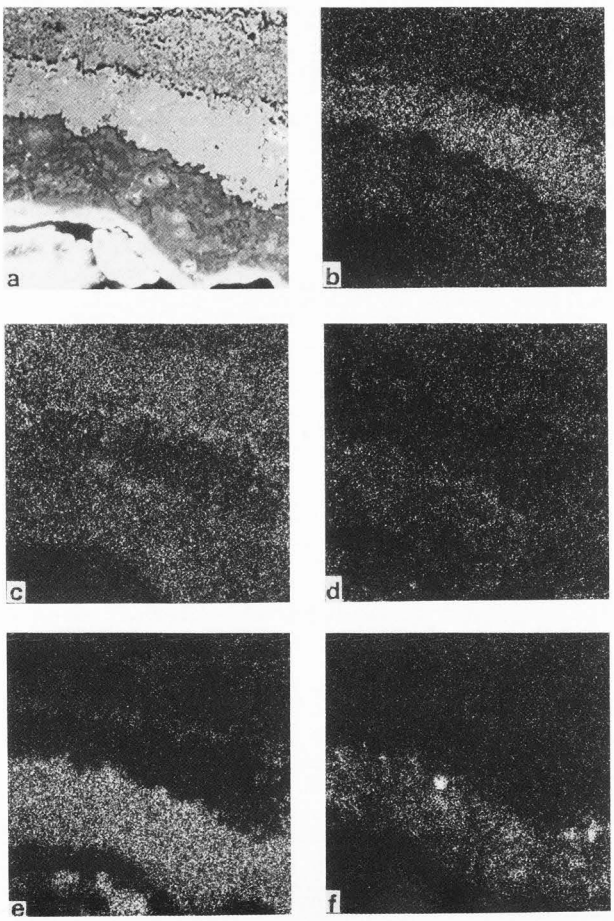

Fig. 28. Specimen of blade (cf. Fig. 27), SEM/WDX-investigation. a) SE-image, border base material/coating, concentration maps: b) Ni; c) Cr; d) Al; e) O; f) S.

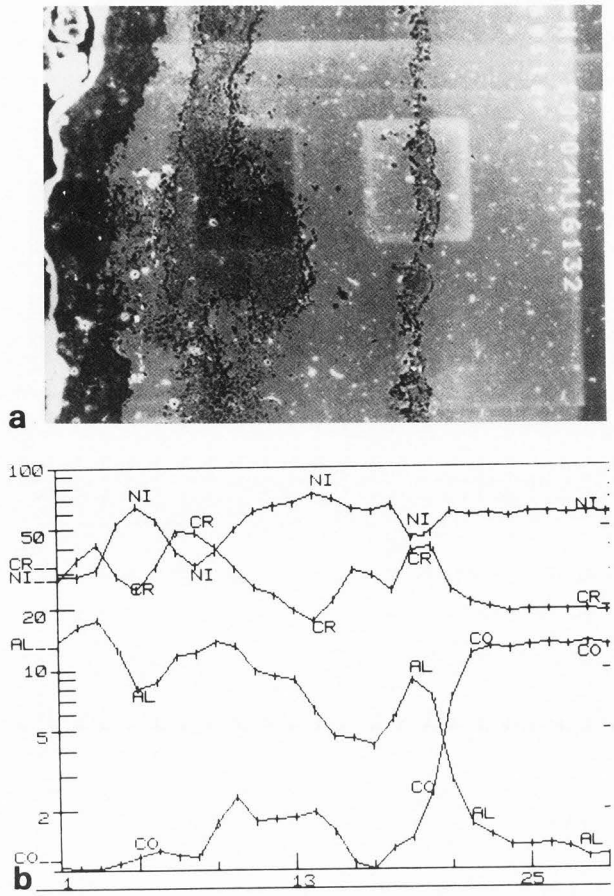

Fig. 29. "Integral layer profile analysis", specimen as in Fig. 27. a) SE-image; b) corresponding concentration profiles of Cr, Ni, Al and Co.

Conclusions

The economical and technical objective to increase the lifetime of gas turbine blades - including a higher efficiency by increasing the gas inlet temperature - requires at least two steps. First: the selection of a material which is resistant against HTC under the given conditions for as long as possible. Second: protective coatings to prevent the corrosion attack for a long time, this means that the penetration of the coating takes place very late.

Figure 31 - a modification of a diagram proposed by Felix [11] - shows the problem in a schematic view. The upper zone "repair/exchange", defined by a certain amount of material loss (waste), will be reached very late by a material with excellent HTC-resistance; this time will be prolonged considerably by selection of a coating with sustained protective effect.

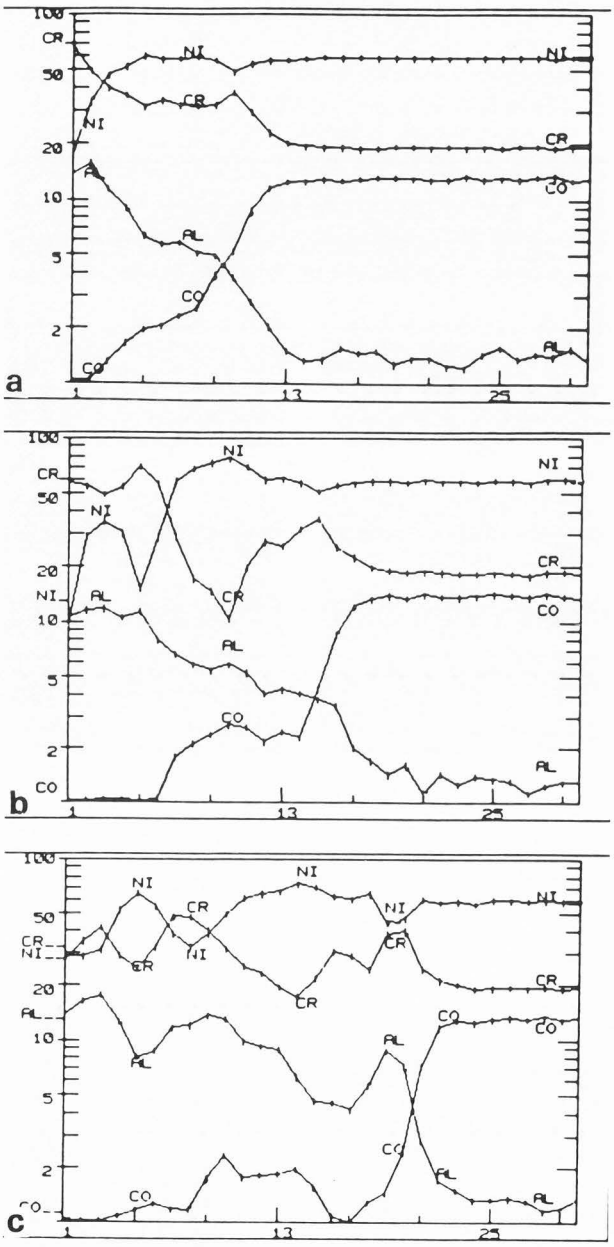

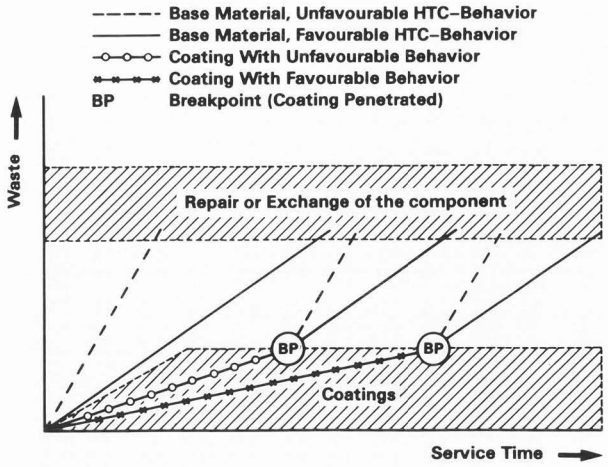

Fig. 31. Lifetime amelioration by coatings (schematic view). (above)

Fig. 30. SEM/WDX-investigation of Udimet 520 + NiCrAlY-coating, comparison of concentration profiles ("integral layer profile analysis". a) As-delivered; b) HTC-laboratory test, 750°C/10,000 h, ash, air + 0.03 Vol.% SO_2/SO_3; c) 20,000 h operation, 750°C, natural gas. (left)

This problem will require a lot of intensive investigations in the future; the procedure of comparing laboratory and engine tests will be a suitable technique. Scanning electron microscopy and related techniques, such as AES, SIMS, ESCA, TEM and STEM techniques, will have a major role to clarify complicated processes in the microscopic zones.

Further Developments and Future Prospects

In the near future, the required properties for gas turbine blades will be still fulfilled by the HT-materials and coatings described in the chapters above. But in order to ameliorate the efficiency of the engine, to achieve a greater output with lower amounts of primary energy, the gas inlet temperatures will increase far above the ranges used today. Thus, the complex Ni- and Co-base superalloys will be replaced by new materials which are in development for some years; also a lot of national and international research programs have been started in this field (e.g., COST-programs of the European Communities).

In Figure 32, a future prospect is given in a schematic representation, showing the increase in yield strength against the expected year of success. The development will start with directionally solidified alloys (polycrystalline - already used), proceed to single crystal material (used in aircraft engines), followed by directionally solidified eutectic alloys, oxide-disperse materials, intermetallic phases of different composition, and

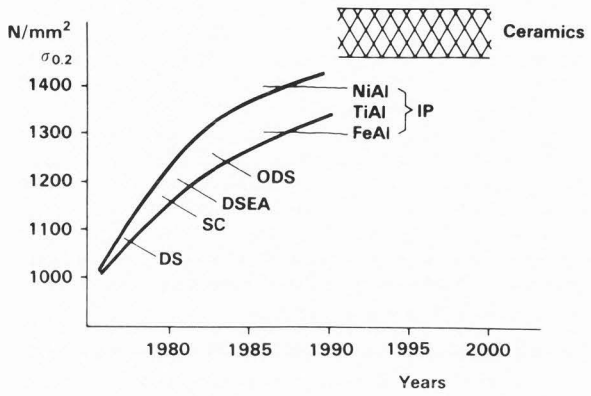

Fig. 32. Operation ranges of high temperature materials (after Dienst [10]).

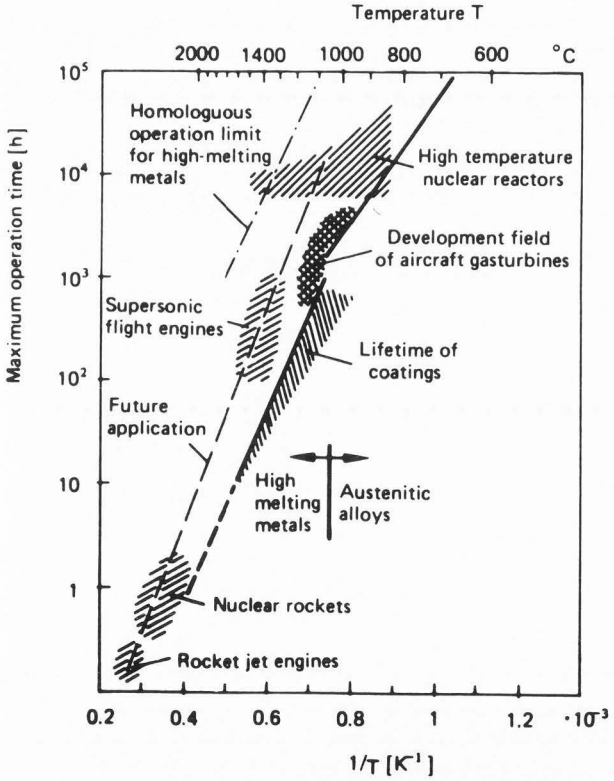

Fig. 33. Upper limit of operation times in oxidizing atmosphere, f (T), (after Dienst [10]).

- at higher temperatures and yield strengths - by ceramic materials; however, the problem with ceramics is and will be the missing ductility.

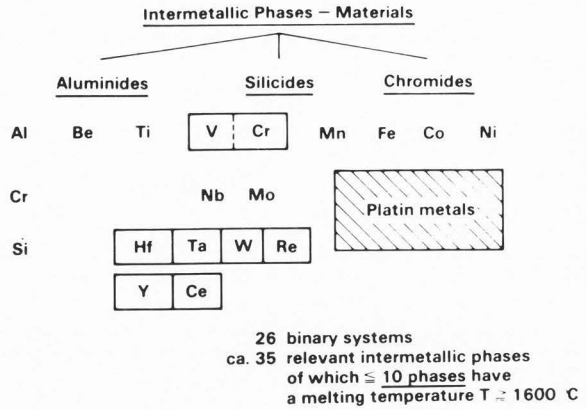

Fig. 34. HT-materials of intermetallic phases (IP). Possible combinations.

In spite of amelioration by construction (better cooling systems aso.), the representation in Figure 33 (after Dienst [10]) gives an overview of the upper limit of operational lifetime as a function of operation temperature; here, the usable temperature range for coatings is limited at 1400°C, and that requires thermal barrier coatings (with Pt as a possible barrier material), which are to develop or to ameliorate. In the immediate future, intermetallic phase (IP) materials seem to have an excellent potential; Figure 34 gives a schematic survey on those IP materials which are already in use or in test programs (Materials Research Program of the Federal Republic of Germany, e.g.).

Summary

The phenomenon "High Temperature Corrosion" has been discussed from different aspects, taking gas turbine blades as an example. The importance of the problem was the reason for extensive investigations either in laboratory tests under defined conditions or in practical operation (e.g., exposure and subsequent examination of various materials and coatings in a gas turbine over longer periods of operation).

The behaviour of different coatings was compared, showing chromium diffusion coatings to be advantageous under the given conditions. Plasma spray coatings were examined at elevated temperatures (up to T = 900°C); the analytical method "integral layer profile analysis" was introduced to ameliorate concentration profiles like line-scans. This method is a suitable tool to study the behaviour

of base material/coating systems; as a result, CoCrAlY-coatings cannot be used at about 900°C. In a future prospect, an attempt for the further development of HT-materials is made; those materials can be single crystals, directionally solidified eutectic alloys and, at last, ceramics. This work demonstrates the extent to which metallurgical investigations with SEM and related techniques can contribute to the evaluation of coating effectiveness under operating conditions. Such investigations influence the selection of materials and coatings with the aim of increasing output, economy and durability of the plant.

Acknowledgements

The authors thank Mrs. Hilde Krüger, KWU Laboratories Mülheim, for the extensive microprobe investigations and Mrs. Rita Wolters and Mr. Willi Slotty, KWU Laboratories Mülheim, for the excellent metallographic work. The authors feel very indebted to Professor K.H. Kloos and Dr. J. Granacher, Technische Hochschule Darmstadt, Federal Republic of Germany, Institut für Werkstoffkunde (Institute for Materials Technology), for carrying out the creep rupture tests in hot gas test rigs. Also, the authors thank their colleagues Mr. F. Schmitz. Dr. N. Czech and Mr. K.-H. Keienburg for helpful discussions, and Mr. E. Ilgenstein for his intensive assistance in preparing this work.

References

1. Adam P, Johner G, Wilms V (1983) Mikroanalytische Untersuchungen von plasmagespritzten Heißgaskorrosionsschutzschichten (Microanalytical investigations of plasma sprayed hot gas corrosion coatings). Metall 37, Nr. 4, 359-364.

2. Becker B (1979) Erprobung einer neuen Leistungsklasse für Gasturbinen mit Grundlast über 100 MW (Testing a new power class for gas turbines with a basic load of more than 100 MW). Motortechnische Zeitschrift 40, 247-249.

3. Beltran AM (1970) Die Oxidations- und Hochtemperaturkorrosionsbeständigkeit von Kobalt-Superlegierungen (The oxidation and hot corrosion resistance of cobalt superalloys). Cobalt, Vol. 46 (March), 3-13.

4. Betz W, Huff H, Track W (1976) Zur Bewertung von Schutzschichten gegen Heißgaskorrosion an Gasturbinenschaufeln (The evaluation of coatings against hot gas corrosion of gas turbine blades). Werkstoffe und Korrosion, Vol. 5, 161-196.

5. Betz W (1978) Mechanical performance of materials under high temperature corrosion conditions, High Temperature Alloys for Gas Turbines, 409-422. Applied Science Publishers, London, Coutsouradis D, Felix P, Fischmeister H, Habraken L, Lindblom Y, Speidel MO (eds.)

6. Betz W (1978) Profile of Requirements for Protective Coatings Against High Temperature Corrosion and Some Experience with their Behaviour in Service, Materials and Coatings to Resist High Temperature Corrosion. Applied Science Publishers, London, Holmes DR, Rahmel R (eds.).

7. Boettger H. Umland F (1974) Untersuchungen zur Hochtemperaturkorrosion durch Chloride (Investigations on High Temperature Corrosion by Chlorides). Werkstoffe und Korrosion 25, Vol. 1, 805-816.

8. Chiang KT, Pettit FS, Meier GH (1981) Low temperature hot corrosion. National Association of Corrosion Engineers (NACE), San Diego, CA, 518-530.

9. Davis FN, Grinell CE (1982) Engine Experience of Turbine Rotor Blade Materials and Coatings. ASME Paper 82-GT-244, Am. Soc. of Mechanical Engineers, NY.

10. Dienst W (1984) Hochtemperaturwerkstoffe (High temperature materials). Werkstofftechnik, Verlagsgesellschaft Karlsruhe.

11. Felix P (1977) Korrosion und Korrosionsschutz in modernen stationären Gasturbinen (Corrosion and corrosion protection in modern stationary gas turbines). BBC-Mitteilungen, Vol. 64, 40-46.

12. Fitzer E, Mäurer HG (1978) Spontane Ausbildung von Diffusionsbarrieren in Alitierschichten auf Nickellegierungen (Spontaneous formation of diffusion barriers in aluminide coatings on nickel alloys). Archiv für Eisenhüttenwesen 49, Vol. 2, 95-99.

13. Goebel JA, Pettit FS, Goward GW (1973) Hot Corrosion Mechanism in Stationary Gas Turbines. Deposition and Corrosion in Gas Turbines. Applied Science Publishers, London, Hard AG, Cutler AJB (eds.), 96-114.

14. Goward GW (1985) Low-temperature hot corrosion in gas turbine: A review of causes and coatings therefore. Turbomachinery International (May-June), 24-28.

15. Jackson MR, Rairden JR (1977) Protective Coatings for Superalloys and the Use of Phase Diagrams, Proceedings of Workshop held at National Bureau of Standards, Gaithersburg MD, NBS-STP 492, NBS, Washington D.C., 423-439.

16. Keienburg KH, Eßer W, Deblon B (1985) Refurbishing procedures for blades of large stationary gas turbines. Materials Science and Technology (August), Vol. 1, 620-628.

17. Marijnissen GH, van Schaik T (1980) Study of Gas Phase Coating Mechanism, Final Report COST 50 (Round II) NL 3, Nr. R 80-66. Commission of European Community, Brussels (Belgium).

18. Pettit FS, Goward GW (1982) Coatings for High Temperature Applications. Applied Science Publishers, London, Lang E (ed.).

19. Rahmel A, Schmidt M (1976) Untersuchungen über das Zusammenwirken von mechanischer Belastung und von Korrosion durch Sulfatschmelzen bei definierten elektrochemischen Potentialen (Studies on the synergism of mechanical stress and corrosion by sulfate melts at defined electrochemical potentials). Final Report COST 50 Program, Project D 1/9. Commission of European Community, Brussels (Belgium).

20. Rahmel A (ed.) (1983) Aufbau von Oxidschichten auf Hochtemperatur-Werkstoffen und ihre technische Bedeutung (Symposium) (Forming oxide layers on high temperature materials and their technical importance). Dt. Ges. f. Metallkunde, Oberursel, ISBN 3-88355-065-5.

21. Saunders SRI (1984) Effects of trace elements and environmental impurities on oxidation and hot-corrosion characteristics of superalloys. Metals Technology (Oct.), Vol. 11, 465-473.

22. Schmitt-Thomas KHG, Johner G, Meisel H (1981) Einfluß von Heißgasatmosphären auf Zeitstandverhalten und Gefüge einer mit Beschichtung versehenen Nickelbasislegierung (Influence of hot gas atmospheres on creep rupture behaviour and structure of coated nickel base alloys). Werkstoffe und Korrosion 32, 255-264.

23. Schmitz F (1980) Langzeit-Korrosionsversuche mit und ohne mechanische Beanspruchung an hochwarmfesten Legierungen für die Schaufeln von ortsfesten Gasturbinen großer Leistung (Long time corrosion testing with and without mechanical stress of high temperature alloys for blades of land based gas turbines with high output). VDI Res. Report Technol. Forschung und Entwicklung - Technol. Research and Development, Fed. Min. Res. and Technol. (BMFT), 79-106.

24. Schmitz F, Slotty W, Thien V (1984) Oberflächenschutzschichten gegen Hochtemperaturkorrosion von Schaufelwerkstoffen stationärer Gasturbinen (Coatings against High Temperature Corrosion of blade materials of stationary gas turbines). Metall 38, Vol. 3, 204-213.

25. Thien V, Schieferstein U, Voss W (1977) Mikroanalytische Untersuchungen hochwarmfester Legierungen für Gasturbinenschaufeln (Microanalytical investigations of high temperature superalloys for gas turbine blades). Mikrochimica Acta, Suppl. 7, Springer Wien New York, 389-403.

26. Thien V, Voss W, Schmitz F (1981) Hochtemperaturkorrosion an hochwarmfesten Werkstoffen - metallographische, rastermikroskopische und mikroanalytische Untersuchungen (Hot corrosion on high temperature materials, metallographic, scanning electron microscopic and microanalytical tests). Proc. 10. Sitzung AK Rastermikroskopie, Dt. Verb. für Materialprüfung (DVM), German Association for Materials Testing, 257-278.

27. Thien V, Voss W, Schmitz F (1982) High Temperature Corrosion on High Temperature Materials. Z. f. Werkstofftechnik 13, 338-347.

28. Thien V, Schmitz F, Slotty W, Voss W (1984) Metallurgical Investigations with Scanning Electron Microscopy and Related Techniques on High Temperature Materials and Coatings against High Temperature Corrosion. Scanning Electron Microsc. 1984; IV: 1629-1642.

29. Thien V, Schmitz F, Slotty W, Voss W (1984) Metallkundlich-mikroanalytische Untersuchungen der Wirkung von Schutzschichten gegen Hochtemperaturkorrosion von Gasturbinenschaufelwerkstoffen (Metallurgical-microanalytical investigations of coatings against high temperature corrosion of gas turbine blade materials). Fresenius Z. Anal. Chem. No. 319, 646-654.

30. Thien V, Wolters R, Voss W (1985) Phase Characterization in High Temperature Alloys with Scanning Electron Microscopy and Related Analytical Techniques. Scanning Electron Microsc. 1985; IV: 1501-1507.

31. Thien V (1985) Selection and Qualification Tests of High Temperature Materials by Special Microanalytical Methods. Mikrochimica Acta, Suppl. 11, 229-261.

32. Thien V, Schmitz F, Wolters R, Voss W (1986) Untersuchung der Schutzschicht von Hochtemperatur-Werkstoffen nach erosiv-korrosivem Angriff (Investigation of the coating of high temperature materials after erosive-corrosive attack). Beitr. eletronenmikroskop. Direktabb. Oberfl. (BEDO) 19, 269-282.

33. Umland F, Voigt HP (1970) Die Rolle der Alkalisulfate bei der Hochtemperaturkorrosion (The influence of alkali sulphates on hot corrosion). Werkstoffe und Korrosion 4, 254-263.

34. Wickert K (1968) Das Verhalten von Staub und Verbrennungsgas in Dampferzeugern (Behaviour of dust and combustion gases in steam generators). VGB-Mitteilungen 3, 149-154.

Discussion with Reviewers

H. Hantsche: Do you see any possibilities to stop the undesired diffusion processes by establishing diffusion barriers?
Authors: Yes, in principle. There have been developed some diffusion barrier systems (cf. references!); the problem is 1. the adherence on the base material, 2. the long-time resistance of these barriers. Research is going worldwide.

H. Hantsche: Your future prospects mention ceramics and its disadvantages. What do you think of compound material, already used in aircraft industry which overcome many of the limitations inherent in ceramic material?
Authors: Those materials are under consideration and will have a growing potential in the next decades. At time, the dimensions of blades of large stationary gas turbines require properties which cannot be fulfilled by available materials.

C.A. Mozden: The criterion chosen for the column diagram (in Figure 8) was the time at which macroscopic penetration was visible. Is this an industry standard or is this your standard for this paper?
Authors: Mainly our standard, by practical reasons (i.e., when revising the engine during an inspection). But some other companies are using the same method.

H. Hantsche: Figure 13b - what does Al-peak mean?
Authors: It belongs to the coating process; Al is enriched here because it is deposited first.

H. Hantsche: Are the given values (Figure 13b, e.g.) the mean average of the 30 measurements?
Authors: Yes, as described.